Propulsion and Energy Forum
July 25-27, 2016, Salt Lake City, UT
52nd AIAA/SAE/ASEE Joint Propulsion Conference

Linear Burn Rates of Monopropellants for Multi-Mode Micropropulsion

Alex J. Mundahl[1], Steven P. Berg[2] and Joshua L. Rovey[3]
Missouri University of Science and Technology, Rolla, Missouri 65409

Multi-mode micropropulsion is a potential game-changing technology enabling rapidly composable small satellites with unprecedented mission flexibility. Maximum mission flexibility requires propellant that is shared between the chemical and electric propulsion systems. Previous research has identified a promising monopropellant that is both readily catalytically exothermically decomposed (chemical mode) and electrosprayable (electric mode). In this work the linear burn rate of this monopropellant is determined to aid design of the microtube catalytic chemical thruster. A pressurized fixed volume reactor is used to determine the linear burn rate. Benchmark experiments use a 13 molar mixture of hydroxylammonium nitrate and water, and show agreement to within 5% of literature data. The multi-mode monopropellant is a double-salt ionic liquid consisting of 41% 1-ethyl-3-methylimidazolium ethyl sulfate and 59% hydroxylammonium nitrate by mass. At the design pressure of 1.5 MPa the linear burn rate of this propellant used for designing the muli-mode propulsion system is 22.8 mm/s. Based on this result, the minimum flow rate required is 0.25 mg/s for a feed tube with a 0.1 mm inner diameter and 2500 mg/s for a feed tube with a 10 mm inner diameter.

Nomenclature

r_b	=	linear burn rate
Δx	=	change in position
Δt	=	change in time
A_c	=	cross-sectional area of propellant container
m_p	=	mass of propellant used
ρ_p	=	density of propellant used

I. Introduction

MULTI-mode propulsion is the use of two or more separate propulsive modes on a single spacecraft. Recently proposed systems make use of a high-specific impulse, usually electric mode, and a high-thrust, usually chemical mode. This can be beneficial in two primary ways: an increase in mission flexibility,[1-5] and the potential to design a more efficient orbit using the two systems compared to a single chemical or electric mode.[6-9] The increase in mission flexibility is achieved due to the availability of the two differing propulsive manuevers to the mission designer at any point during the mission. This allows for drastic changes to the mission thrust profile at virtually any time before or even after launch without the need to integrate an entirely new propulsion system. Additionally, it has been shown that, under certain mission scenarios, it is beneficial in terms of spacecraft mass savings, or deliverable payload, to utilize separate high-specific impulse and high-thrust propulsion systems even if there is no shared hardware or propellant.[6,8,10] However, even greater mass savings can potentially be realized by using a shared propellant and/or hardware even if the thrusters perform lower than state-of-the-art in either mode.[11,12] In order to realize the complete potential of a multi-mode propulsion system, it is necessary to utilize one shared propellant for

[1] Undergraduate Research Assistant, Aerospace Plasma Laboratory, Mechanical and Aerospace Engineering, 160 Toomey Hall, 400 W. 13th Street, Student Member AIAA.
[2] Post Doctoral Research Assistant, Aerospace Plasma Laboratory, Mechanical and Aerospace Engineering, 160 Toomey Hall, 400 W. 13th Street, Student Member AIAA.
[3] Associate Professor of Aerospace Engineering, Mechanical and Aerospace Engineering, 292D Toomey Hall, 400 W. 13th Street, Associate Fellow AIAA.

both modes; this allows for a large range of possible maneuvers while still allowing for all propellant to be consumed regardless of the specific choice or order of maneuvers.[13] Two propellants have been developed that can function as both a chemical monopropellant and an electrospray propellant.[12] These monopropellants have been previously synthesized and assessed for thermal and catalytic decomposition within a microreactor,[14] and for performance in an electrospray emitter.[15] One of the monopropellant combinations, a mixture of 1-ethyl-3-methylimidazolium ethyl sulfate ([Emim][$EtSO_4$]) and hydroxylammonium nitrate (HAN), has also been further analyzed to determine its decomposition characteristics, specifically on relevant catalytic surfaces.[14,16] This paper further studies the characteristics of the [Emim][$EtSO_4$]-HAN monopropellant by determining the linear burn rate of this propellant at pressures relevant to typical monopropellant thruster operation.[17]

Recent efforts in developing propellants for space vehicles have focused on finding a high-performance, low-toxicity propellant replacement for traditional, but highly toxic options. Hydrazine has been chosen for use in gas generators and spacecraft monopropellant thrusters due to its storeability and favorable decomposition characteristics in providing relatively high performance.[18] However, hydrazine is difficult from a handling perspective since it is highly toxic. A large amount of the research toward a hydrazine replacement is focused on energetic ionic liquids. An energetic ionic liquid is a molten salt with an energetic functional group capable of rapid exothermic decomposition. Energetic salts that have been studied for such purposes include ammonium dinitramide (ADN), hydrazinium nitroformate (HNF), and hydroxylammonium nitrate (HAN).[18-22] Typically, these salts are mixed with compatible fuels to improve the performace characteristics of the produced propellant. However, the high combustion temperatures for these energetic monopropellants have been the main limitation in their practical use in spacecraft thrusters, but recent research in thermal management and materials have mitigated some issues, and multiple flight tests are scheduled, or have already been conducted.[22-25] These propellants perform well in chemical thrusters, but they are fundamentally unable to perform as an electrospray propellant due to their water content or other volatile component. To overcome this, the previously described monopropellants were developed, synthesized, and shown to be capable of high performance in an electrospray thruster.[12,14]

Small spacecraft have seen a growth in popularity, specifically microsatellites (10-100 kg) and nanosatellites (1-10 kg), including the subset of cubesats. Many different types of thrusters have been proposed to meet the stringent mass and volume requirements placed on spacecraft of this type. Electrospray propulsion systems are good options for micropropulsion, and have been selected for such applications.[26,27] Many different chemical propulsion systems have also been proposed, including a chemical microtube.[28-30] This propulsion system utilizes a heated tube with a typical diameter of 1 mm or less that could consist of a catalytic surface material. Additionally capillary type emitters used for an electrospray propulsion system can be roughly the same diameter tube, and there is therefore no fundamental reason why this geometry could not be shared within a multi-mode propulsive system.[31,32]

The linear burn rate of the propellant used at the thruster anticipated operating pressures is a useful parameter in the design of the system, both for thruster operation and flashback prevention. The linear burn rate has been studied previously for monopropellants, including HAN-based monopropellants.[33-35] This paper presents results on the experimental determination and assessment of the linear burn rate characteristics of the [Emim][$EtSO_4$]-HAN propellant at various pressures through the use of a pressurized strand burner setup. These measurements, taken together, can be used to aid in the design and optimization of a catalytic microtube thruster. Section II describes the setup of the experiment, Section III presents the results of the experiment, Section IV discusses the results including relevant development or selection of microtube thruster parameters, and Section V presents the conclusions of this study.

II. Experimental Setup

The pressurized linear burn rate studies performed here are similar to those described in previous studies utilizing HAN-based propellants and nitromethane.[36,37] In a pressurized linear burn rate experiment a sample of propellant is ignited and combusts within a known sealed volume. Pressure within the volume is measured as a function of time with the propellant burn time determined based on discontinuities within the pressure profile corresponding to the initiation and extinguishment of combustion. Using the measured burn time, known mass of propellant, and known geometry of the propellant sample holder, it is possible to calculate the linear burn rate of the propellant.

The experimental setup is shown in Figure 1, and a schematic of the experiment is shown in Figure 2. The propellant sample holder is shown in Figure 3. The propellant sample holder is a 5.9-mm-internal-diameter quartz tube that is 45 mm tall. It was sized to allow for roughly 1 ml of propellant to be used for each test. The propellant holder is epoxied to the bottom of a brass cap. The brass cap also serves as the electrical feedthrough for two wires that provide electrical power to ignite the propellant. Propellant is ignited by applying voltage to and thus resistively

heating nickle-chromium (nichrome) wire. For each test two pieces of equal length 30 gauge nichrome wire are twisted together and soldered to the electrical leads within the brass cap. The nichrome wires are then bent and submerged within the propellant. The brass cap with propellant holder attaches to a four-way cross through which it is connected to a large (~0.7L) cylinder volume. This additional volume acts to minimize the change in pressure within the setup as the propellant burns. Also connected to the setup are a pressure transducer, a pressure gauge, a hand valve, and two gas feedthroughs. The pressure transducer is an Omega PX309-300A5V with an absolute pressure range of 0 to 300 psi, and it monitors the pressure versus time within the volume. The pressure gauge is a Zenport DPG500 Zen-Tek Dry Air Pressure Gauge. The hand valve is used to vent the system following a completed test. The hand valve opens the volume to atmosphere and a venting system consisting of a fan and hose expels the combustion gases from the building. One of the gas feedthroughs is used to evacuate the setup with a mechanical vacuum pump, and the second is used to repressurize the evacuated system with inert argon to the desired test pressure.

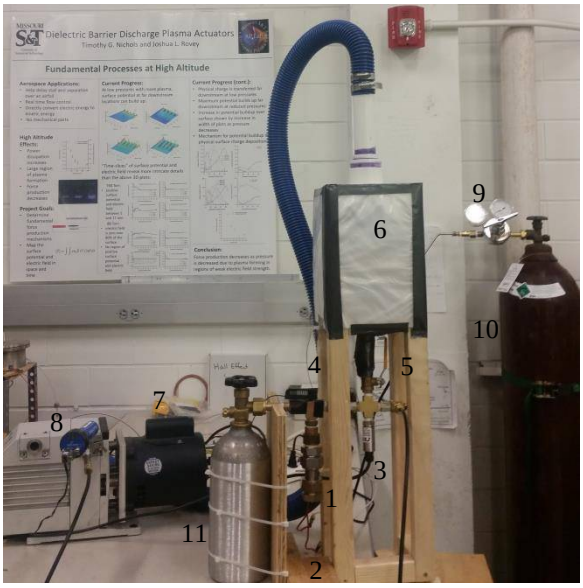

Components:
1. Cap with Propellant Holder
2. Wire Feedthroughs for Power
3. Pressure Transducer
4. Mechanical Pressure gauge
5.Hand Valve
6.Venting System
7. Mechanical Vacuum Pump
8. Digital Pressure Gauge
9. Pressure Regulator
10. Argon Tank
11. Large Stainless Steel Cylinder

Figure 1. Linear Burn Rate Experimental Setup

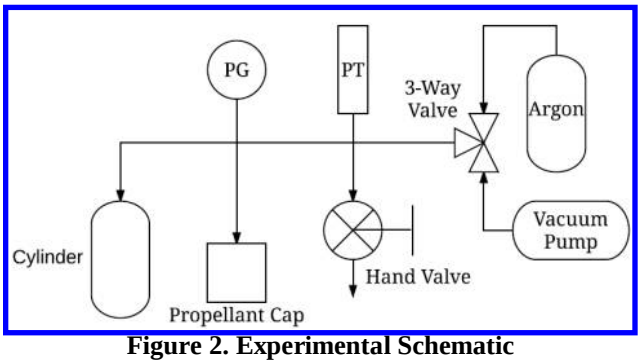

Figure 2. Experimental Schematic

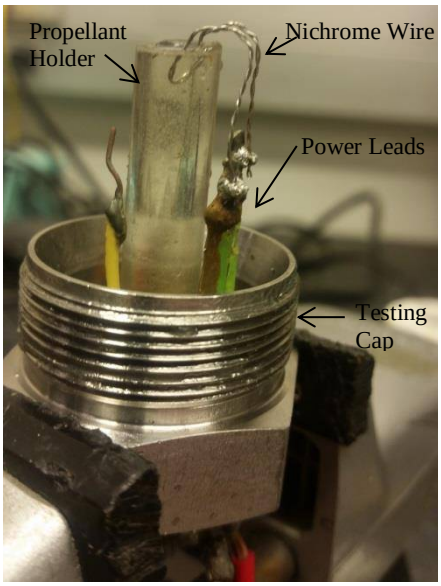

Figure 3. Testing Cap Setup

The experimental procedure includes weighing the empty test cap mass and syringe filled with propellant. A Torbal AGC500 mass balance with 0.001 grams resolution is used to determine the mass of the sample. Then the propellant is added to the propellant holder, the nichrome igniter wire attached and submerged in the propellant. Then the test cap is attached to the setup and the volume evacuated using the mechanical rough pump to a pressure of 10 Torr (1.3 kPa). After reaching this reduced pressure the volume is repressurized using inert argon to the desired pressure level for the test. Results presented below are for a pressure range of 0 to 200 psig (0.1 – 1.5 MPa) in 50 psi (0.34 MPa) increments. Once the desired pressure is reached the oscilloscope is triggered to record data, and power provided to the system. For each test 8.5 A of current is provided to the twisted nichrome wires via voltage from a power supply. This current magnitude causes the wires to break after heating the propellant. This magnitude of current provides similar breaking times to those within previous studies.[38] A Tektronix DPO 2024 Digital Phosphor Oscilloscope records the pressure transducer output and power supply voltage. The measured pressure versus time, along with the known mass of propellant, and known geometry of the propellant sample holder, is used to determine the propellant linear burn rate.

Benchmark tests using 13M HAN-water are conducted, followed by tests using the [Emim][$EtSO_4$]-HAN monopropellant. The monopropellant has a mixture ratio of 41% [Emim][$EtSO_4$] to 59% HAN by mass because this is the formulation envisioned for use within a multi-mode propulsion system and the focus of the previous research.[12-15,17,39] The process for synthesizing this propellant is described in detail within previous studies.[14,15] The 13M HAN-Water solution was prepared by drying 24% by wt. HAN-Water solution as described previously, then adding distilled water to the solid HAN for the final solution. Relevant propellant characteristics are given in Table 1.

Table 1. Propellant Characteristics

Propellant Tested	Density (g/cm^3)	Mass HAN (%)	Mass Other (%)
HAN-Water	1.57	80	20
[Emim][$EtSO_4$]-HAN	1.53	59	41

III. Results

The results from the linear burn rate experiments are presented here. Initially benchmark tests are performed with 13M HAN-water propellant at a pressure of 200 psig. These tests show good agreement with literature. Then tests with the energetic ionic liquid monopropellant [Emim][$EtSO_4$]-HAN are performed at pressures of 50, 100, 150, and 200 psig. All of the tests performed within this studied use about 1 ml of propellant, with the exact mass of propellant used in each test determined by measuring the weight of the sample.

A. Calculating Linear Burn Rate

Linear burn rate can be readily calculated for a propellant with constant cross-section. The linear burn rate is the change in length/height of propellant over a time period, as described in Equation 1. Previous studies have shown that the burn time can be determined from the pressure rise due to burning the propellant within a fixed volume.[36,37]

$$r_b = \frac{\Delta x}{\Delta t} \tag{1}$$

The change in length/height can be determined from the other known properties of the setup, according to Equation 2. Specifically the known propellant mass, propellant density, and diameter of the sample holder are used. The density of the 13M HAN-water is 1.57 g/cm^3 and the density of the [Emim][$EtSO_4$]-HAN is 1.53 g/cm^3. The sample holder diameter is 5.9 mm. The mass of propellant used for each test is measured using a mass balance. Combining Equations 1 and 2 results in Equation 3, which is used to calculate the linear burn rate of propellant.

$$\Delta x = \frac{4m_p}{\pi \rho_p D_c^2} \tag{2}$$

$$r_b = \frac{4m_p}{\pi \rho_p D_c^2 \Delta t} \tag{3}$$

B. Benchmark HAN-Water Results

Tests are performed with a 13.0M HAN-water mixture and compared with previous results by Katsumi, et. al.[34] to benchmark and validate the experimental setup and test procedure. A typical pressure profile during a test of the HAN-water is given in Figure 4. There is a clear discontinuity in the pressure profile at -4.7 sec indicating the

ignition and initiation of combustion of the propellant. The end of combustion is the discontinuity at -1.1 sec, where the pressure profile then returns to the exponential decreasing trend. This decrease in pressure depicts the heated combustion products cooling after all of the propellant has been consumed. The difference between these two points is the burn time for the sample. The burn time determined from similar results for multiple samples is given in Table 2. Also given in Table 2 are the measured mass of the sample and the corresponding calculated burn rate for the HAN-water tests. The average burn rate for the 80% HAN-water mixture at 200 psig (1.5 MPa) is 8.1±1.0 mm/s.

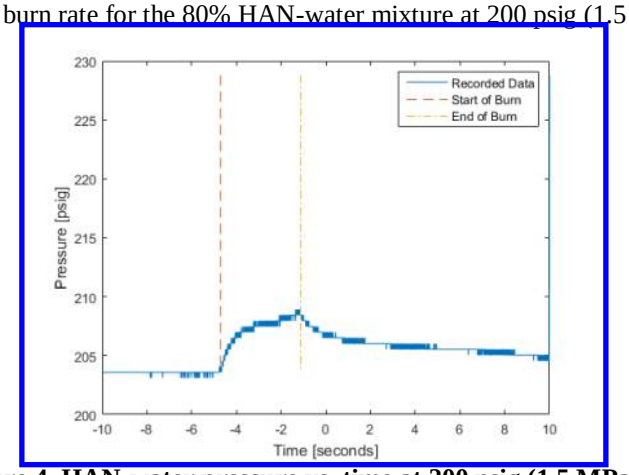

Figure 4. HAN-water pressure vs. time at 200 psig (1.5 MPa)

Table 2. HAN-water results at 200 psig (1.5 MPa)

Test Number	Burn Time (s)	Mass Used (g)	Burn Rate (mm/s)
1	4.3	1.53	9.1
2	4.4	1.30	7.7
3	3.6	1.05	7.5

Results from previous experiments are plotted alongside the average burn rate measured here in Figure 5. Previous work by Katsumi et.al.[34] measured the burn rate of 80, 82.5, 85, and 90% HAN-water mixtures from 1-10 MPa. For a 80% HAN-water mixture at 200 psig (1.5 MPa), Katsumi et.al.[34] measure a burn rate of 8.4 mm/s. This result is within 0.3 mm/s (5%) of the 8.1 mm/s burn rate measurd here.

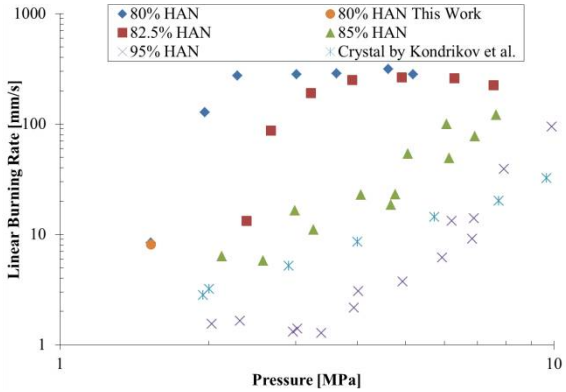

Figure 5. Comparison of linear burning rate measured here with previous results for 80 - 95% aqueous HAN solutions from reference [34]

C. [Emim][$EtSO_4$]-HAN Monopropellant

An example pressure profile for the [Emim][$EtSO_4$]-HAN monopropellant at 200 psig is shown in Figure 6. This figure displays the start and end of the burn time, and the pressure change throughout the test. For this propellant, there is a clear increase in pressure indicating the time when the propellant sample ignites at 1.1 sec. The [Emim][$EtSO_4$]-HAN monopropellant has an almost instantaneous spike in pressure up to 290 psig, and further testing is required in order to determine the reasoning for such an event, as the current data set does not have precise enough resolution to determine if this is a physical shock, or electrical glitch. The pressure remains high until 2.0 sec

followed by a noticeable drop-off as the propellant sample is fully consumed and the pressure begins to stabilize back to equilibrium. The burn time determined from similar plots for each sample, along with the measured mass and calculated burn rate are displayed in Table 3. All of these tests use a fully submerged nickel-chromium wire setup, except for the last data point displayed. An illustration of these different locations within the sample holder is shown in Figure 7.

This last point used a partially dipped nickel-chromium wire setup, where the nickel-chromium wire was only submerged just below the top surface of propellant. This was done in order to examine the significance of the amount of nickel-chromium wire to the linear burn rate of [Emim][$EtSO_4$]-HAN monopropellant within this experimental setup, and this will be discussed within the discussions section. The average linear burn rate for [Emim][$EtSO_4$]-HAN monopropellant is 46.2±7.1 mm/s, 22.6±4.6 mm/s, and 51.6±0.5 mm/s for the, 200, 150, and 100 psig pressures with a fully submerged nichrome ignitor wire, respectively. For a partially dipped ignitor wire, the linear burn rate for is 22.6 mm/s at 200 psig. The uncertainty is reported as the 95% confidence interval of the data.

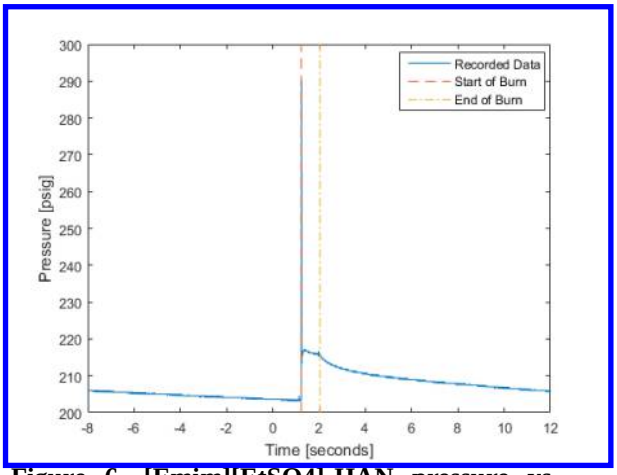

Figure 6. [Emim][EtSO4]-HAN pressure vs. time at 200psig (1.5 MPa)

Table 3. [Emim][$EtSO_4$]-HAN results at multiple pressures

	Burn Time (s)	Mass Used (g)	Burn Rate (mm/s)
		200 psi	
1	0.81	1.27	41.7
2	0.85	1.55	49.5
3	0.51	0.92	47.8
		150 psi	
4	1.42	1.33	24.9
5	1.72	1.31	20.3
		100 psi	
6	0.66	1.29	51.9
7	0.59	1.14	51.4
		50 psi	
8	1.15	1.34	30.9
9	0.62	1.25	53.8
		200 psi with partially dipped Nichrome Wire	
10	1.12	0.98	22.6

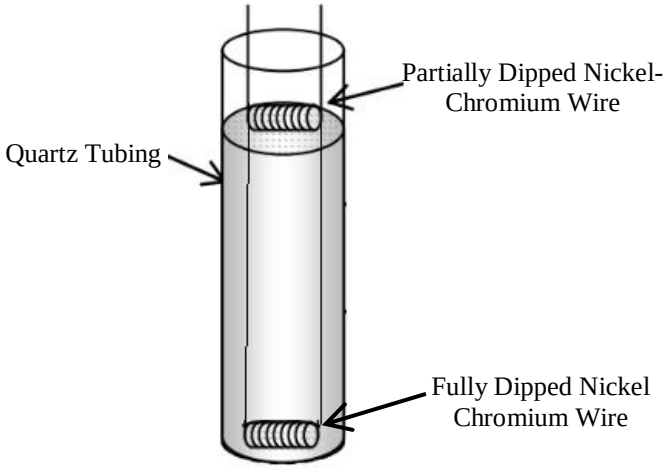

Figure 7. Fully vs. Partially Dipped Nickel-Chromium Wire Locations

D. Power Supplied to Each Test

The initial and final time power is supplied to the system is recorded. These data are useful in exploring correlations between the time power is supplied to the system and the measured linear burn rate. The initial and final time power is supplied to the system is compared with the beginning and ending time of each respective propellant burn, and these data are shown in Table 4 for the HAN-Water tests and Table 5 for the [Emim][$EtSO_4$]-HAN tests. The initial time power is applied to the system is taken as the origin, and the results shown are the elapsed time. There are two sets of results, one from each data table, where the nickel-chromium wire did not break. To differentiate these from the other data points, these data have a (M). These data sets will be compared in the discussions section below.

Table 4. 13.0 M HAN-Water Power Supplied and Burn Time results at multiple pressures

	Time of Start of Burn (s)	Time of End of Burn (s)	End of Power Supplied (s)
1	0.375	4.682	1.603
2	0.708	5.060	1.606
3	2.199	5.709	12.441 (M)

Table 5. [Emim][EtSO4]-HAN Power Supplied and Burn Time results at multiple pressures

	Time of Start of Burn (s)	Time of End of Burn (s)	End of Power Supplied (s)
		200 psi	
1	1.223	2.035	1.343
2	0.130	0.643	2.102
3	0.029	0.864	1.336
		150 psi	
4	0.103	1.524	1.082
5	0.132	1.846	0.953
		100 psi	
6	0.150	1.856	1.623
7	0.592	1.183	2.126
		50 psi	
8	0.216	1.428	1.726
9	1.583	2.199	16.041 (M)
		200 psi with partially dipped Nichrome Wire	
10	0.275	1.396	1.724

The results from Table 4 for HAN-Water show that the first two experimental runs had burn times lasting 3 to 3.5 seconds past the end of power supplied to the system. This is different from the last set of data where the power had to be manually disconnected (i.e., the ignitor wire did not break). The results shown in Table 5 for [Emim][$EtSO_4$]-HAN are similar. Two tests at 200 psi, the 200 psi test with partially dipped nickel-chromium wire, one 100 psi test, and both tests for 50 psi have burn times that are smaller than the time power is applied to the system. The other tests have varying burn times where the system does not have any power.

IV. Discussion

Results from the preceding section are discussed, including insights for the development of a microtube thruster. The effect of pressure on the burn rate will be discussed first, followed by the effect of these results on the design of a multi-mode propulsion system.

A. Pressure Trend for [Emim][$EtSO_4$]-HAN Burn Rate

An interesting component of the results shown in Table 3 is the noticeable large decrease in burn rate at 150 psi compared to the values at 200 psi and 100 psi. When compared to the previous work performed on HAN-Water, this noticeable decrease could indicate another discrete change in slope for the linear burning rate as shown in 80%, 82.5%, and 95% HAN by weight results within Figure 5. This, however, has never been shown within previous literature at these pressures, and, from Figure 5, the trend one would expect as pressure is decreased is for the burn rate to only reduce slightly. This change could also be due to a general plateau trend where the linear burning rate stays close to the same over a particular pressure regime, but at individual testing locations they undulate across the average burn rate. This may be seen in 80%, 82.5% and 95% HAN by weight within Figure 5 as well, but without a physical explanation for such a trend. However, from Table 5, it is seen that at the 100 psia and below test cases the total time during which power is applied is greater than the burn time. Or stated another way, the nicrome wire does not break before the propellant is consumed. It is likely, then, that the heated wire drives the decomposition of the propellant throughout the entire burn duration without igniting the propellant. Because of this, the burn rate data garnered at these pressures is likely not indicative of the burn rate of quiescent propellant. The most likely trend, then, is a relatively sharp decrease in slope as pressure is decreased from 200 psia as is seen with the HAN/Water blends in Figure 5 at the lowest pressures. More testing within the 100 psi to 200 psi pressure regime for [Emim][$EtSO_4$]-HAN, and other monopropellants, is required in order to clarify this change in slope.

Along with these results, a test was performed at 200 psig with only a small amount of nickel-chromium wire submerged into the test setup to determine how much this would affect the results. The reasoning behind fully submerging the nickel-chromium wire was that previous studies with other propellants, like nitromethane, had submerged a significant amount of their nickel-chromium wires in order to evenly heat the propellant. Within these past experiments, the propellant burns past the end of power being supplied to the system, but in instances in both the HAN-Water results, and the [Emim][$EtSO_4$]-HAN results, it was shown that there were cases of tests having completed burns before the nickel-chromium wire disconnected power from the system. These instances could suggest excess energy provided to the chemical reaction, further increasing the linear burn rate. Furthermore, for HAN-based propellants, nickel acts as a catalyst and could also contribute to erroneously enhanced burn rate. As the results from Table 4 show both cases within the results for HAN-Water, and with these same results being used to confirm the experimental setup, it was determined that this correlation between the burn time and the time of power provided to the system do not actually significantly affect the linear burn rate of the HAN/Water blend. There are significantly smaller burn times for the [Emim][$EtSO_4$] –HAN results, however.

The other aspect of this question, the affects of the length of nickel-chromium wire used, also had to be discussed, which is why this particular test was run. In previous experimentation,[37] a correlation was made between the amount of wire exposed to propellant and the linear burn rate. This correlation stated that the more exposed wire, the faster the linear burn rate. The test with partially dipped nickel-chromium wire confirms this correlation seeing this final test was almost 50 percent less than the previously determined average burn rate at the same pressure. This difference is taken into consideration when discussing the impact of linear burn rate results on the design of a catalytic microtube thruster in the next section of this discussion. Seeing this result is absent of both preheat and catalytic effects, it was determined that the linear burn rate of 22.8 mm/s would be more representative of a propellant feed system during nominal operation which is not externally heated and ideally made of a compatible material. The burn rate obtained with the fully dipped nicrome wire may be more representative of the propellant flow in the thruster, where the incoming propellant is heated fairly uniformly.

B. Impact of Burn Rate Results on Catalytic Microtube Microthruster Design

The linear burn rate, traditionally determined and used for solid propellant motor design, is a useful parameter in the design of chemical monopropellant thrusters. The most obvious application to thruster design is in the prevention of flashback into the feed system or propellant tank. Since the goal of the sample holder in the linear burn rate experiments is to minimize the effect of heat transfer in the quenching of the propellant decomposition reaction, the linear burn rate results can be used to obtain an upper bound on the required minimum feed rate in a tube or other geometry. This is an upper bound because as tube diameter is decreased heat transfer to the wall becomes more significant, causing the reaction to quench absent any tube preheat or catalytic effects. The linear burn rate obtained from experiment can then be used to define a minimum flow rate as a function of tube diameter to feed the propellant to the thruster at a rate greater than the burn rate of the propellant.

The minimum flow rate, as described in the previous paragraph, is calculated for tube inner diameters of 0.1 to 10 mm and is shown in Fig. 8. The two lines shown in the figure correspond to the burn rates determined for the [Emim][$EtSO_4$]-HAN propellant at 200 psia with the nicrome wire fully dipped into the sample holder and partially dipped into the propellant, 49.5 mm/s and 22.8 mm/s respectively. As previously discussed, the lower number likely represents a more accurate measure of the burn rate of this propellant, absent catalytic and preheat effects. Using this number, the minimum flow rate required is 0.25 mg/s for a tube of 0.1 mm inner diameter and 2500 mg/s for a tube of 10 mm inner diameter. For a microtube type thruster, which does not include a nozzle, the specific impulse of this propellant is 170 seconds. This corresponds to a minimum thrust level of 0.4 mN for a 0.1 mm inner diameter tube and 4.16 N for a 10 mm diameter tube. Or, stated in a way more representative of design selection, if a thruster of 4.16 N thrust is desired, the feed tube must be a maximum of 10 mm inner diameter. The fully dipped nicrome results are included in Fig. 8 to illustrate what may happen if the feed tube is catalytic or is heated to high temperature. The minimum mass flow rate required for the 10 mm diameter tube is now 5500 mg/s, or 2.2 times that of the unenhanced burn rate case, which is why great care must be taken in the design and selection of tube material and thermal standoffs.

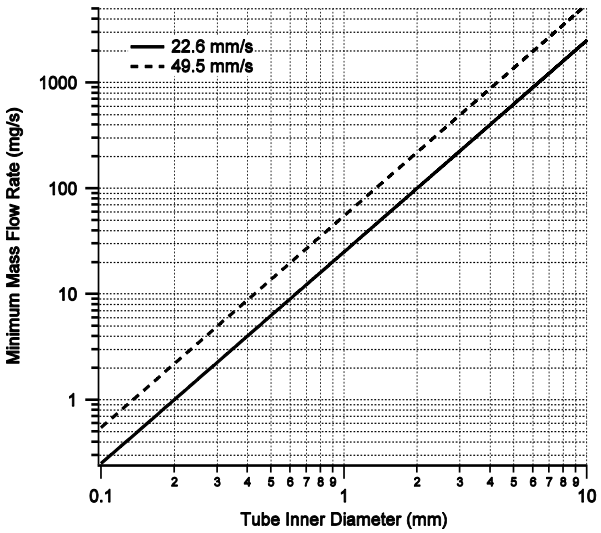

Figure 8. Minimum required propellant mass flow rate to prevent flashback into feed system for [Emim][EtSO4]-HAN propellant.

V. Conclusion

From the results provided and the following discussion, it was determined that the linear burn rate of the specified [Emim][$EtSO_4$]-HAN monopropellant mixture using the fully dipped nickel-chromium wire at 200 psig is between 39.7 and 52.6 mm/s with 95% confidence, while the linear burn rate for partially dipped nickel-chromium wire is 22.8 mm/s. Seeing this result is absent of both preheat and catalytic effects, it was concluded to be more representative of a microtube thruster during nominal operation where the microtube is not externally heated, except to initialize the burn. From this result, it was concluded that the minimum flow rate required for a 0.1 mm microtube is 0.25 mg/s, and 2500 mg/s for a tube of 10 mm inner diameter. These discoveries should help improve the results of the multi-mode propulsion system under design, and improve the system final performance.

Acknowledgments

Support for this work was provided through the NASA Marshall Space Flight Center, NASA grant NNM15AA09A, and the Air Force University Nanosatellite Program through the Utah State University Research Foundation, grant CP0039814. Additionally, A. J. Mundahl thanks the Soffen Space Travel Grant for travel support. The authors would also like to thank the researchers of the Aerospace Plasma Laboratory for their assistance throughout this experiment, and providing insightful information. Finally, the authors thank the technicians within the department machine shop for their assistance in the manufacturing process of this experiment.

References

[1]Rexius, T., and Holmes, M., "Mission Capability Gains from Multi-Mode Propulsion Thrust Profile Variations for a Plane Change Maneuver," *AIAA Modeling and Simulation Technologies Conference*, AIAA Paper 2011-6431, 2011.

[2]Haas, J. M., and Holmes, M. R., "Multi-Mode Propulsion System for the Expansion of Small Satellite Capabilities," Air Force Research Laboratory, Rept. NATO MP-AVT-171-05, 2010.

[3]Donius, B. R. and Rovey, J. L., "Ionic Liquid Dual-Mode Spacecraft Propulsion Assessment," *Journal of Spacecraft and Rockets*, Vol. 48, No. 1, 2011, pp. 110-123.

[4]Berg, S. P., and Rovey, J. L., "Assessment of High-Power Electric Multi-Mode Spacecraft Propulsion Concepts," *33rd International Electric Propulsion Conference*, IEPC-2013-308, 2013.

[5]Berg, S. P., and Rovey, J. L., "Assessment of Multi-Mode Spacecraft Micropropulsion Systems," *Journal of Spacecraft and Rockets*, Vol. No. 2016, pp. in review; also AIAA Paper 2014-3758, July 2014.

[6]Kluever, Craig A., "Spacecraft Optimization with Combined Chemical-Electric Propulsion," *Journal of Spacecraft and Rockets*, Vol. 32, No. 2, 1994, pp. 378-380.

[7]Kluever, Craig A., "Optimal Geostationary Orbit Transfers Using Onboard Chemical-Electric Propulsion," *Journal of Spacecraft and Rockets*, Vol. 49, No. 6, 2012, pp. 1174-1182.

[8]Oh, David Y., Randolph, Thomas and Kimbrel, Scott, "End-to-End Optimization of Chemical-Electric Orbit Raising Missions," *Journal of Spacecraft and Rockets*, Vol. 41, No. 5, 2004, pp. 831-839.

[9]Oleson, Steven R., Myers, Roger M., Riehl, John P. and Curran, Francis M., "Advanced Propulsion for Geostationary Orbit Insertion and Nort-South Station Keeping," *Journal of Spacecraft and Rockets*, Vol. 34, No. 1, 1997, pp. 22-28.

[10]Mailhe, L. M., Heister, S. D., "Design of a Hybrid Chemical/Electric Propulsion Orbital Transfer Vehicle," *Journal of Spacecraft and Rockets*, Vol. 39, No. 1, 2002, pp. 131-139.

[11]Donius, Brian R. and Rovey, Joshua L., "Ionic Liquid Dual-Mode Spacecraft Propulsion Assessment," *Journal of Spacecraft and Rockets*, Vol. 48, No. 1, 2011, pp. 110-123.

[12]Berg, Steven P. and Rovey, Joshua L., "Assessment of Imidazole-Based Energetic Ionic Liquids as Dual-Mode Spacecraft Propellants," *Journal of Propulsion and Power*, Vol. 29, No. 2, 2013, pp. 339-351.

[13]Berg, Steven P. and Rovey, Joshua L., "Assessment of High-Power Electric-Mode Spacecraft Propulsion Concepts," *33rd International Electric Propulsion Conference*, 2013.

[14]Berg, Steven P. and Rovey, Joshua L., "Decomposition of Monopropellant Blends of Hydroxylammonium Nitrate and Imidazole-Based Ionic Liquid Fuels," *Journal of Propulsion and Power*, Vol. 29, No. 1, 2013, pp. 125-135.

[15]Berg, Steven P., Rovey, Joshua L., Prince, B. P., Miller, S. W. and Bemish, R. J., "Electrospray of an Energetic Ionic Liquid Propellant for Multi-Mode Micropropulsion Applications," *51st AIAA/ASME/SAE/ASEE Joint Propulsion Conference*, 2015.

[16]Berg, S. P., and Rovey, J. L., "Decomposition of a Double Salt Ionic Liquid Monopropellant on Heated Metallic Surfaces," *52nd AIAA/ASME/SAE/ASEE Joint Propulsion Conference & Exhibit*, to be presented, 2016.

[17]Berg, Steven P., "Development of Ionic Liquid Multi-Mode Spacecraft Micropropulsion Systems," Dissertation, Mechanical and Aerospace Department, Missouri University of Science and Technology, 2015.

[18]Sutton, G. P. and Biblarz, *Rocket Propulsion Elements*, 7th, Wiley, New York, 2001.

[19]Amariei, Dan, Courtheoux, Laurence, Rossignol, Sylvie, Batonneau, Yann, Kappenstein, Charles, Ford, Mark and Pillet, Nicolas, "Influence of the Fuel on Thermal and Catalytic Decompositions of Ionic Liquid Monopropellants," *41st AIAA/ASME/SAE/ASEE Joint Propulsion Conference and Exhibit*, 2005.

[20]Anflo, K., Gronland, T. A., Bergman, G., Johansson, M. and Nedar, R., "Towards Green Propulsion for Spacecraft with AND-Based Monopropellants," *38th AIAA/ASME/SAE/ASEE Joint Propulsion Conference and Exhibit*, 2002.

[21]Slettenhaar, B., Zevenbergen, J. F., Pasman, H. J., Maree, A. G. M. and Moerel, J. L. P. A., "Study on Catalytic Ignition of HNF Based Non Toxic Monopropellants," *39th AIAA/ASME/SAE/ASEE Joint Propulsion Conference and Exhibit*, 2003.

[22]Anflo, K., Persson, S., Thormahlen, P., Bergman, G. and Hasanof, T., "Flight Demonstration of AND-Based Propulsion System on the PRISMA Satellite," *42nd AIAA/ASME/SAE/ASEE Joint Propulsion Conference and Exhibit*, 2006.

[23]McLean, C. H., Deininger, W. D., Joniatis, J., Aggarwal, P. K., Spores, R. A., Deans, M., Yim, J. T., Bury, K., Martinez, J., Cardiff, E. H., Bacha, C. E., "Green Propellant Infusion Mission Program Development and Technology Maturation," *50th AIAA/ASME/SAE/ASEE Joint Propulsion Conference*, AIAA Paper 2014-3481, 2014.

[24]Anflo, K, Persson, S., Thormahlen, P., Bergman, G., and Hasanof, T., "Flight Demonstration of ADN-Based Propulsion System on the PRISMA Satellite," *42nd AIAA/ASME/SAE/ASEE Joint Propulsion Conference & Exhibit*, AIAA Paper 2006-5212, 2006.

[25]Anflo, K., Mollerberg, R., "Flight Demonstration of New Thruster and Green Propellant Technology on the PRISMA Satellite," *Acta Astronautica*, Vol. 65, No. 9-10, 2009, pp. 1238-1249.
[26]Chiu, Y., Dressler, A., "Ionic Liquids for Space Propulsion", *Ionic Liquids IV: Not Just Solvents Anymore*, Vol. 975, American Chemical Society, Washington, D. C., 2007, Ch. 10.
[27]Gamero-Castano, M., "Characterization of a Six-Emitter Colloid Thruster Using a Torsional Balance," *Journal of Propulsion and Power*, Vol. 20, No. 4, 2004, pp. 736-741.
[28]Mento, C. A., Sung, C-J., Ibarreta, A. F., Schneider, S. J.,, "Catalyzed Ignition of Using Methane/Hydrogen Fuel in a Microtube for Microthruster Applications," *Journal of Propulsion and Power*, Vol. 25, No. 6, 2009, pp. 1203-1210.
[29]Boyarko, G. A., Sung, C-J., Schneider, S. J.,, "Catalyzed Combustion of Hydrogen-Oxygen in Platinum Tubes for Micro-Propulsion Applications," *Proceedings of the Combustion Institute*, Vol. 30, No. 2, 2005, pp. 2481-2488.
[30]Volchko, S. J., Sung, C-J., Huang, Y., Schneider, S. J.,, "Catalytic Combustion of Rich Methane/Oxygen Mixtures for Micropropulsion Appications," *Journal of Propulsion and Power*, Vol. 22, No. 3, 2006, pp. 684-693.
[31]Alexander, M. S., Stark, J., Smith, K. L., Stevens, B., Kent, B., "Electrospray Performance of Microfabricated Colloid Thruster Arrays," *Journal of Propulsion and Power*, Vol. 22, No. 3, 2006, pp. 620-627.
[32]Berg, S. P., and Rovey, J. L., "Design and Development of a Multi-Mode Monopropellant-Electrospray Micropropulsion System," *30th AIAA/USU Conference on Small Satellites*, to be presented, 2016.
[33]Chang, Y-P, "Combustion Behavior of HAN-Based Liquid Propellants," Mechanical Engineering, Pennsylvania State University, 2002.
[34]Katsumi, T., Hori, K., Matsuda, R., Inoue, T., "Combustion Wave Structure of Hydroxylammonium Nitrate Aqueous Solutions," *46th AIAA/ASME/SAE/ASEE Joint Propulsion Conference*, AIAA Paper 2010-6900, 2010.
[35]Homan-Cruz, G. D., McCown III, K. W., Petersen, E. L., "Effects of Nano-scale Additives and Methanol on the Linear Burning Rates of Aqueous HAN Solutions," *50th AIAA/ASME/SAE/ASEE Joint Propulsion Conference*, AIAA Paper 2014-3566, 2014.
[36]Warren, William Charles, "Experimental Techniques for the Study of Liquid Monopropellant Combustion," Mechanical Engineering, Texas A&M University, 2012.
[37]Warren, W. C., McCown, K., and Peterson, E. L., "Experimental Techniques for the Study of Ionic Liquid Combustion at High Pressure," *Spring Technical Meeting the Central States Section of the Combustion Institute*, 2012.
[38]Warren, William Charles, "Experimental Techniques for the Study of Liquid Monopropellant Combustion," Office of Graduate Studies of Texas A&M University, Texas A&M, 2012.
[39]Berg, Steven P. and Rovey, Joshua L., "Assessment of Multi-Mode Spacecraft Micropropulsion Systems," *50th AIAA/ASME/SAE/ASEE Joint Propulsion Conference*,
[40]McCown, K., Demko, Andrew R. and Petersen, Eric L., "Effects of Methanol and Fumed Silica on the Linear Burning Rates of Aqueous Hydroxylammonium Nitrate," *10th International Symposium on Special Topics in Chemical Propulsion & Energetic Materials (10-ISICP)*, 2014.